SMARTER

SMAll RuminanTs breeding for Efficiency and Resilience

Research and Innovation action: H2020 – 772787
Call: H2020-SFS-2017-2
Type of action: Research and Innovation Action (RIA)
Work programme topic: SFS-15-2016-2017
Duration of the project: 01 November 2018 – 31 October 2022

Scientific manuscript and source code of prediction models for trade-offs under nutritional and infectious challenges

Frédéric Douhard[1], Carole Moreno-Romieux[1], Rachel Rupp[1], Marcelo Gindri[2], Laurence Puillet[2], Nicolas C. Friggens[2], Andréa B. Doeschl-Wilson[3]

[1] GenPhySE, Université de Toulouse, INRAE, ENVT, 31326, Castanet Tolosan, France ; [2] Université Paris Saclay, INRAE, AgroParisTech, UMR 0791 MoSAR, 16 rue Claude Bernard, 75005 Paris, France ; [3] The Roslin Institute, University of Edinburgh, Midlothian, EH25 9RG, UK

* Deliverable leader – Contact: frederic.douhard@inrae.fr

DELIVERABLE D3.3

Workpackage N°3

Due date: M48

Actual date (original version): 23/12/2022

Date of revised version: 23/08/2023

Dissemination level: Public

This project has received funding from the European Union's Horizon 2020 research and innovation programme under grant agreement No 772787

About the SMARTER research project

SMARTER will develop and deploy innovative strategies to improve Resilience and Efficiency (R&E) related traits in sheep and goats. SMARTER will find these strategies by: i) generating and validating novel R&E related traits at a phenotypic and genetic level ii) improving and developing new genome-based solutions and tools relevant for the data structure and size of small ruminant populations, iii) establishing new breeding and selection strategies for various breeds and environments that consider R&E traits.

SMARTER with help from stakeholders chose several key R&E traits including feed efficiency, health (resistance to disease, survival) and welfare. Experimental populations will be used to identify and dissect new predictors of these R&E traits and the trade-off between animal ability to overcome external challenges. SMARTER will estimate the underlying genetic and genomic variability governing these R&E related traits. This variability will be related to performance in different environments including genotype-by-environment interactions (conventional, agro-ecological and organic systems) in commercial populations. The outcome will be accurate genomic predictions for R&E traits in different environments across different breeds and populations. SMARTER will also create a new cooperative European and international initiative that will use genomic selection across countries. This initiative will make selection for R&E traits faster and more efficient. SMARTER will also characterize the phenotype and genome of traditional and underutilized breeds. Finally, SMARTER will propose new breeding strategies that utilise R&E traits and trade-offs and balance economic, social and environmental challenges.

The overall impact of the multi-actor SMARTER project will be ready-to-use effective and efficient tools to make small ruminant production resilient through improved profitability and efficiency.

Table of contents

1 Summary

Resource allocation models, embedded into mechanistic host-pathogen interaction models can provide powerful decision support tools to be used by scientists, farmers and animal breeders for managing trade-offs and optimising resilience and efficiency (R&E) of animals under a variety of challenging conditions. The objective of this study was to provide mechanistic models to simulate potential trade-offs during infectious or nutritional challenges at the animal level. Here we describe a mechanistic host-pathogen interaction model for gastro intestinal infections in sheep based on resource allocation to analyse trade-offs during **infectious** and **nutritional** challenges. The model has been calibrated with data from the parasite resistance Romane sheep line experiments conducted in SMARTER. Nutritional costs associated with host resistance to gastro-intestinal parasite infections have been estimated and used to predict and manage trade-offs. Based on our experimental data, we conclude that a positive energy cost of parasite resistance is likely. This energy cost can lead to a genetic trade-off between parasite resistance and fat deposition in lambs and may thus constrain breeding strategies in particular when feed energy is scarce. This deliverable D3.3 reports the work done in the form of a scientific manuscript and supplies the correponding code in Appendix1. A short description of complementary analysis on a second allocation model developed for goat is given in Appendix2.

2 Introduction

The magnitude of nutritional costs of mounting and maintaining an immune response have been subject of much debate among immunologists and nutritional scientists (Coop and Kyriazakis, 1999; Lochmiller and Deerenberg, 2000; Colditz, 2007). Such costs are also thought to be of primary importance in the evolution of life-history strategies as they provide the basis for resource allocation trade-offs between immune defences and other fitness components such as growth and reproduction (Sheldon and Verhulst, 1996). Thus, estimating these costs is also vital for devising effective practical solutions to combat infectious diseases, including nutritional or breeding strategies.

For gastro-intestinal nematode (GIN) infections in sheep, both nutrient supplementation or selective breeding for increased disease resistance have been described as promising strategy for the sustainable control of parasitism in grazing systems (Stear et al., 2001; Kahn et al., 2003). While promoting a strong immunity to GIN should alleviate parasite-induced damage, a metabolic cost through the diversion of nutrients away from productive functions may incur (Greer, 2008). Accordingly, there may be an optimal level of immunity to select on, which depends on the nutrient allocation and on the costs of immunity (Bishop and Stear, 2003). These would need to be estimated in order to accurately predict selection responses.

In domestic livestock, nutrient allocation theory (Beilharz et al., 1993; Rauw, 2009) forms the basis for modelling the effect of infections on productive performance and health (Doeschl-Wilson et al., 2009). In particular, for gastro-intestinal parasite infections in sheep, such models have demonstrated how trade-offs between production and immunity can arise and can be managed, e.g. through selective breeding or other management solutions (Vagenas et al., 2007a; Laurenson et al., 2012; Saccareau et al., 2016). However, in these models, the predicted effects and optimal solutions depend strongly on

assumptions regarding the nutritional costs associated with host immunity (Doeschl-Wilson et al., 2008).

Yet, obtaining reliable quantitative estimates of such costs from field or experimental data remains difficult (e.g. indirect effects, integrated and organisational characteristics of the immune system with other physiological systems, data).

Our aim was to estimate trade-offs and the energetic cost of mounting an immune response against GIN infection by fitting a mechanistic host-parasite interaction model to experimental data from female lambs from lines divergently selected for their resistance to *Haemonchus contortus* and challenged with this parasite.

3 Material and Methods

3.1 Model description

3.1.1 Model scope and main assumptions

The model scope is a growing non-reproducing sheep fed *ad libitum* with a protein-rich diet, infected with a given dose of third stage infective larvae. It is assumed that energy intake is known.

The model consists of two interacting sub-models representing the host-parasite system and the host energy balance (Fig. 1). The host-parasite system includes two components: the parasite development within the host (from third stage infective larvae LI to reproducing adults Am and Af_{NL}), and the host immune responses against the infection. As for prey-predator models (Fenton & Perkins, 2010), these two components interact dynamically as parasitic load triggers the immune responses which in turn, act on parasite development. The immunological mechanisms by which animals have or acquire resistance to haemonchosis are highly complex and still largely unravelled. Here we defined two latent immune response variables, I_E and I_F acting on two key stages of parasite development, i.e. , I_E limiting the establishment of infective L3 larvae (k_E), and , I_F limiting the reproductive maturation of adult females (k_F)).

For modelling energy balance, we assumed that protein accretion (P) to reach mature size drives body growth and remains unaffected by the infection in its early stages. Excess energy (not used for protein growth or maintenance) then fuels body lipid deposition (L) and leads to change in body condition. Further, just as the synthesis and maintenance of a gram of protein or of lipid has an energy cost (e.g. e_{growth} or e_{dep} in Table 1), we considered that energy costs may also exist for immune responses (e_{I_E} or e_{I_F} in Table 1). However, in contrast to e_{growth} or e_{dep} whose values are relatively well-known from the literature, the values of e_{I_E} or e_{I_F} are unknown.

We aimed to assess if immune responses contribute significantly to the energy balance and to estimate the corresponding energy costs (e_{I_E} and e_{I_F}). For this, the model was fit to experimental data and the quality of fit was assessed both at the individual and at the population level. The detailed methodology of this process is described later (section 3.3). Briefly, at the individual level, blood haematocrit and fecal egg count measures were used to indirectly estimate the magnitudes of the host immune responses I_E and I_F. Simultaneously, data on feed intake, body growth and condition were used to estimate the energy balance of each infected sheep, specifically their protein growth rate. Whilst the magnitude of the host immune response and energy balances vary both over time within an individual, and across individuals, the energy costs associated with the synthesis and maintenance of a gram of protein or of lipid e_{growth} or e_{dep}, and of e_{I_E} or e_{I_F} associated with one unit measure of I_E and I_F,

respectively, were assumed to be equal among individuals. Hence, we repeated individual parameter estimations using different fixed values of e_{I_E} and e_{I_F} and looked for the best average quality of fit at the population level. In particular, if the best fit was obtained without immune energy cost (i.e. using e_{I_E} = 0 and e_{I_F} = 0), this would support the hypothesis that body growth and parasite resistance are independent. In contrast, positive estimates of e_{I_E} or e_{I_F} would support the hypothesis that an energy allocation trade-off occurs between parasite resistance and body condition.

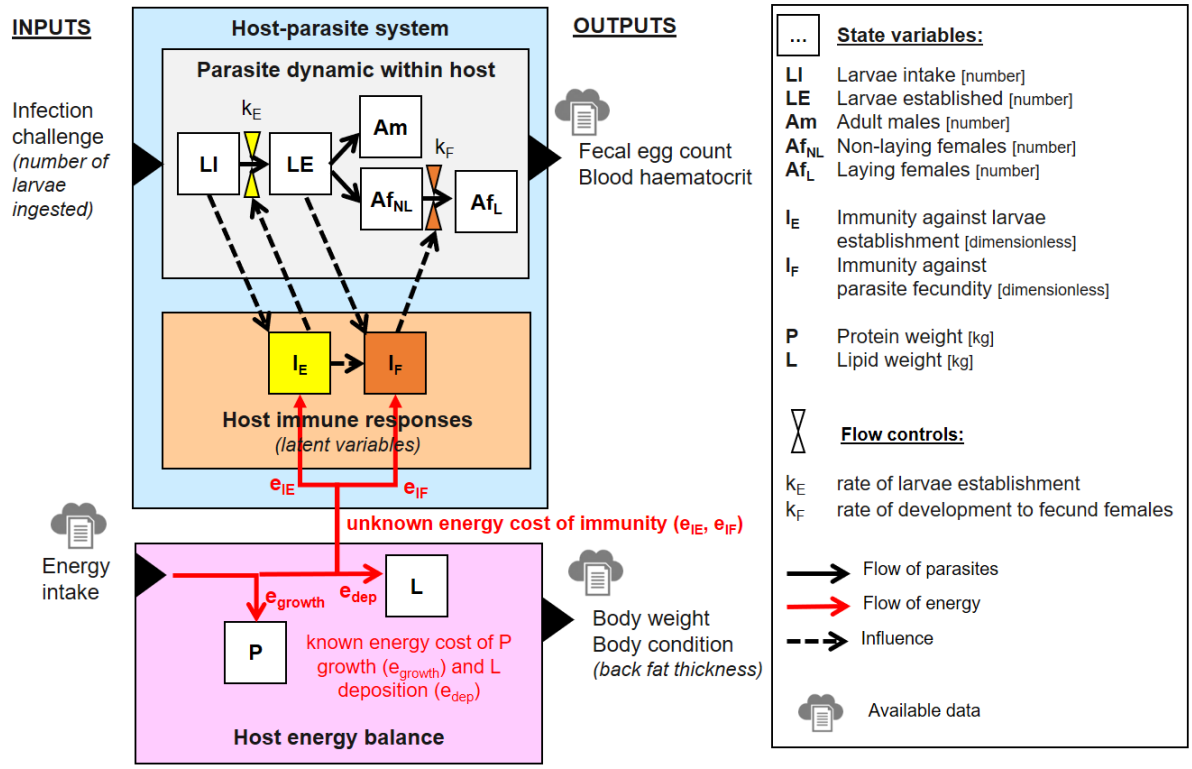

***Figure 1**: Conceptual diagram of the host-parasite model coupled with a model of host energy balance to estimate the energetic cost of immune responses from experimental data.*

3.1.2 Parasites dynamic within-host

The model describes the successive stages of parasite development within the host, from third stage larvae intake (LI) to fourth-stage larvae established in the abomasum (LE), and then from LE to adult fifth stage males (Am) or females (Af). Within females, the transition between non-laying (Af_{NL}) to laying females (Af_L) is represented as this last transition towards the most pathogenic stage largely determines the severity of the infection.

The infection dynamics from the day of inoculation (t = 0 and LI equal to initial dosis LI_0) onwards is described by the following system of ordinary differential equations:

$$\frac{dLI}{dt} = -(\mu_{LI} + k_E) \cdot LI \qquad \text{Eq. (1)}$$

where k_E = 0 if t ≤ τ_{LI}

$$\frac{dLE}{dt} = k_E \cdot LI - (\mu_{LE} + k_A) \cdot LE \qquad \text{Eq. (2)}$$

where k_A = 0 if t ≤ τ_{LE}

$$\frac{dAm}{dt} = p_{Am} \cdot k_A \cdot LE - \mu_{Am} \cdot Am \quad \text{Eq. (3)}$$

$$\frac{dAf_{NL}}{dt} = (1 - p_{Am}) \cdot k_A \cdot LE - (\mu_{Af_{NL}} + k_F) \cdot Af_{NL} \quad \text{Eq. (4)}$$

$$\frac{dAf_L}{dt} = k_F \cdot Af_{NL} - \mu_{Af_L} \cdot Af_L \quad \text{Eq. (5)}$$

where k_E, k_A and k_F are transition rates that determine parasites establishment, development and fecundity and μ parameters are stage-specific mortality rates. Parasite sex is considered when parasites become adults, with p_{Am} indicating the proportion of males. Among the different stages of the parasitic phase, larvae establishment, adult fecundity, and adult mortality are considered to be key targets of the host immune system (Louie et al., 2005). Here we considered immune effects on parasite establishment and fecundity (k_E and k_F) during the first stages of infection that we studied experimentally, and assumed constant mortality rates (μ) and rate of development from L4 to adults (k_A). Establishment rate k_E and female transition rate k_F were considered at maximum values k_{E_0} and k_{F_0} in the absence of any immune effect, and their values were reduced proportionally to the magnitude of specific immune responses I_E and I_F, respectively (further details in section '*Host immune responses*'). Moreover, there is a minimum time τ_{LI} required by ingested third-stage larvae (LI) before reaching host abomasum and establishment, and then a minimum time τ_{LE} to transform into adult fifth stage (Am or Af_{NL}). Thus, k_E and k_A were set to 0 when $t \leq \tau_{LI}$ and when $t \leq \tau_{LE}$, respectively.

Female worm fecundity is closely related to their body size which increases as they growth. To simplify we assumed that Af_{NL} represents an average worm of constant size and fecundity F_0 (i.e. average laying rate) so that the inverse of k_F corresponds to the average development time to reach that size and lay eggs. Thereby, immune influence on k_F controls whole population fecundity, that is the total eggs excretion: $Af_L \cdot F_0$.

In order to fit the model to the experimental data, the dynamics of fecal egg counts (FEC) and blood haematrocit level (HE) was also modelled. Specifically, FEC (eggs number excreted per day and per gram of feces) was defined in relation to the mass of feces produced daily by the host ($Feces$) as follows:

$$FEC = \frac{AF_L \cdot F_0}{Feces} \quad \text{Eq. (6)}$$

with

$$Feces = \frac{FI \cdot DMC_{Feed} \cdot (1 - DMD_{Feed})}{DMC_{Feces}}$$ Eq. (7)

Time change in HE was defined by a constant replication rate α_{HE} and a per capita loss β_{HE} under non-challenging conditions. Under infectious challenge, HE dynamics is also affected by parasitic consumption. Blood haematocrit (HE) was negatively affected by the total number of parasites. This loss was assumed to depend on the parasitic loads associated with the different established parasitic stages (LE, Am, Af_{NL} and Af_L) and on the corresponding stage-specific effects ω:

$$\frac{dHE}{dt} = (\alpha_{HE} - \beta_{HE} \cdot HE) - (\omega_{LE} \cdot LE + \omega_{Am} \cdot Am + \omega_{Af_{NL}} \cdot Af_{NL} + \omega_{Af_L} \cdot Af_L)$$ Eq. (8)

For better ease of parameterization, we defined HE_0 as the equilibrium level of HE that equals β_{HE}/α_{HE} in the absence of infection.
Our model accounts for the fact that HE and FEC dynamics may reflect different biological processes that can be differently controlled by host immunity (e.g. HE can decrease due to some worm burden but this does not necessarily implies a correlated increase in FEC if for instance the host develops a strong anti-fecundity response). Nevertheless, HE and FEC may still be moderately to strongly negatively correlated in accordance with the literature (Vanimisetti et al., 2004).

3.1.3 Host immune response

Effects of the host immune response I_E and I_F on k_E and k_F, respectively, were assumed to follow a sigmoidal pattern (Louie et al., 2005; Fenton and Perkins, 2010), so that at low levels of immunity the responses are relatively inefficient (e.g. in naïve animals) whereas they saturate at high levels, for instance due to time constraints on immune cells to neutralize parasites. In model terms, the maximum ($k_{E_0}$and k_{F_0}), the inflection point ($I_{E_{0.5}}$ and $I_{F_{0.5}}$) and the shape ($\alpha k_E$and αk_F) were determining sigmoidal patterns as follows:

$$k_E(I_E) = \frac{1}{\left(\frac{I_E}{I_{E_{0.5}}}\right)^{\alpha k_E} + 1} \cdot k_{E_0}$$ Eq. (9)

and

$$k_F(I_F) = \frac{1}{\left(\frac{I_F}{I_{F_{0.5}}}\right)^{\alpha k_F} + 1} \cdot k_{F_0}$$ Eq. (10)

The development of immune response against parasite establishment I_E was assumed to be triggered by the intake of L3 larvae (LI). As for the immune effect on parasite we assumed that the increase in the replication rate of I_E according to LI followed a sigmoidal pattern:

$$\frac{dI_E}{dt} = \left(\varphi_{I_E} \cdot \frac{1}{\left(\frac{LI_{0.5}}{LI}\right)^{\alpha I_E} + 1} \cdot I_E \right) - \beta_{I_E} \cdot \left(I_E - I_{E_0}\right) \quad \text{Eq. (11)}$$

The early immune response I_E, in interaction with the number of L4 established larvae (LE) were then assumed to elicit the immune response I_F against the reproduction of adult parasites as follows:

$$\frac{dI_F}{dt} = \left(\varphi_{I_F} \cdot \left(I_E - I_{E_0}\right) \cdot LE\right) - \beta_{I_F} \cdot \left(I_F - I_{F_0}\right) \quad \text{Eq. (12)}$$

Of note, an increase in φ_{I_E} will lead to an increase in I_E (Figure 2A), as well as in I_F in case of positive φ_{I_F} (Figure 2C), respectively. Whereas φ_{I_F} only affect I_F (Figure 2B) and has no effect on I_E, φ_{I_E} has a non-linear effect on I_F (Figure 2C). For low values of φ_{I_E}, I_E increases faster than LE declines (i.e. the product $\left(I_E - I_{E_0}\right) \cdot LE$ increases) whereas for higher values of φ_{I_E}, I_E effectively reduces LE which then subsequently reduces the immune response I_F (as a stimulation of a strong I_F would be pointless). This non-linear effect is more pronounced for higher values of φ_{I_F} (Figure 2C).

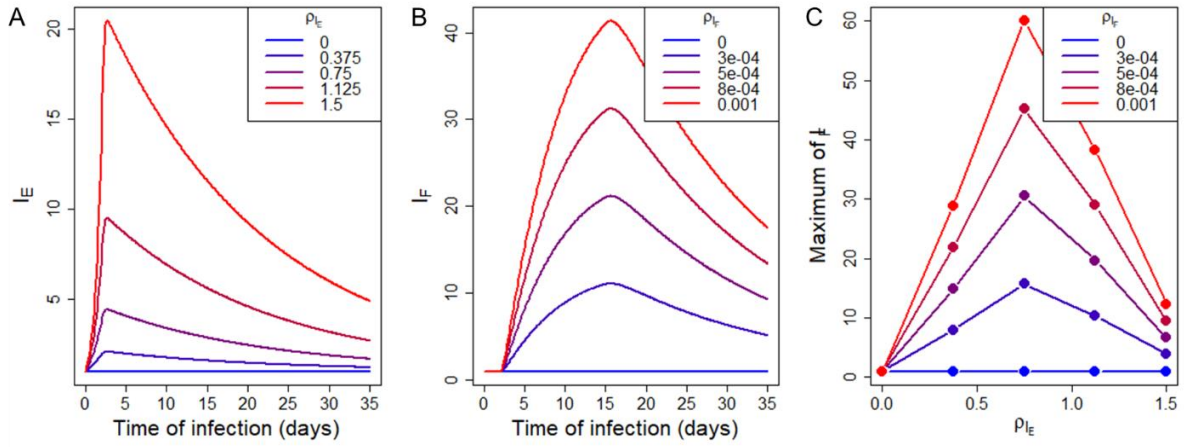

***Figure 2**: Effect of replication rate of each immune response over the course of an infection (effect of φ_{I_E} on I_E) (**A**); effect of φ_{I_F} on I_F (**B**), and indirect effect of φ_{I_E} on I_F depending on φ_{I_F} (**C**) with maximum I_F values observed during infection on the y-axis.*

***Table 1** List of model parameters*

Parameter	Definition	Value	Source
Parasites development			
μ_{LI}; μ_{LE} ; μ_{Am}; $\mu_{Af_{NL}}$; μ_{Af_L}	Mortality rates of LI, LE, and of Am, Af_{NL}, Af_L	0.18; 0.01; 0.015	[1]
p_{A_m}	Proportion of LE that are males (the remaining proportion 1 - p_{A_m} are females)	0.5	assumed
k_{E_0}; k_{F_0}	Maximum transition rates from LI to LE (establishment), and from Af_{NL} to Af_L (fecundity)	2; 0.3	assumed
k_A	Constant transition rate from LE to Am and Af_{NL}	0.62	assumed

Parameter	Definition	Value	Source
τ_{LI} ; τ_{LE}	Minimum time delay (in days) from ingestion to establishment site, and from establishment to emergence	2 15	[1]
F_0	Fecundity rate per capita (number of eggs per day and per adult female)	3000	[2]
ω_{LE} ; ω_{Am}; $\omega_{Af_{NL}}$; ω_{Af_L}	Loss in HE per capita for parasite categories LE, Am, Af_{NL}, and Af_L, respectively	($\times 1^{e\text{-}5}$) 15; 50; 50; 110	[3]
Host immune response			
$I_{E_{0.5}}$; $I_{F_{0.5}}$	Levels of I_E and I_F at which k_E and k_F respectively, are reduced of 50%	5	assumed
αk_E; αk_F	Shape factor of immune effects on k_E and k_F	3	assumed
φ_{I_E}; φ_{I_F}	Per capita replication rate of I_E and I_F, respectively	*assumed to vary between individuals; estimated (individual level)*	
αI_E	Shape factor of parasite effect (LI) on I_E replication	3	assumed
$LI_{0.5}$	Level of LI at which I_E replication is at 50% of its maximum	3000	assumed
I_{E_0}; I_{F_0}	Baseline levels	1	assumed
β_{I_E}; β_{I_F}		0.05	assumed
Host energy balance			
α_{P_m}	Scaling exponent of P_m	0.27	[4]
P_m	Protein weight at maturity	*assumed to vary between individuals; estimated (individual level)*	
L_m	Lipid weight at maturity		
β_P	Relative protein growth rate		
β_{Wool}	Wool growth rate		
e_{growth}; e_{maint}; e_{dep}; e_{mob}	Unitary energy cost (in MJ/kg) of protein growth, protein maintenance, lipid deposition, and lipid mobilization, respectively.	56; 1.63; 50; 39.6	[4]
e_{I_E}; e_{I_F}	Unitary energy cost (in MJ/unit) of immune responses I_E and I_F, respectively	*Estimated (population level)*	
Observed host traits			
γ_{Ash}; γ_{Water}	Fixed ratio Ash:P and Water:P_m, respectively	0.211; 3.25	[4]
α_{Water}	Scaling factor of protein maturity determining the proportion of body water	0.815	[4]
a_{Gut_Fill}; b_{Gut_Fill}	Coefficients to predict Gut_Fill from Feed_Energy	11; 0.467	[5]
a_{BFT} ; b_{BFT} ; c_{BFT}	Coefficients to predict Backfat_Thickness	-4.01; 0.56; 1.52	[6]
DMC_{Feces}	Dry matter content of the feces	0.35	assumed
Diet characteristics			
DMC_{Feed}	Dry matter content of the feed	0.88	known inputs
DMD_{Feed}	Dry matter digestibility of the feed	0.76	
MEC_{Feed}	Metabolizable energy content of the feed (MJ/kg of DM)	7.7	

[1] Smith (1988); [2] Saccareau et al. (2017); [3] Dargie and Allonby (1975); [4] Emmans (1997); Wellock et al. (2004); [5] Laurenson et al. (2011); [6] Macfarlane et al. (2006)

3.1.4 Host energy balance

The host energy balance (EB) was defined as the energy intake minus the sum of the different energy requirements:

$$EB = E_{intake} - (E_{growth} + E_{maint} + E_{immunity}) \quad \text{Eq. (13)}$$

and then determined the rate of lipid (L) deposition or mobilization:

$$\frac{dL}{dt} = e_{dep} \cdot EB \; if \; EB \geq 0 \; and \; \frac{dL}{dt} = e_{mob} \cdot EB \; otherwise. \quad \text{Eq. (14)}$$

This model was based on a previous nutritional growth model (Emmans, 1997; Wellock et al., 2004), except that we added the component $E_{immunity}$ and sought to estimate its parameters based on our experimental data. Specifically, $E_{immunity}$ was considered as a weighted sum of immune responses I_E and I_F:

$$E_{immunity} = e_{I_E} \cdot I_E + e_{I_F} \cdot I_F \quad \text{Eq. (15)}$$

where the weighing factors e_{I_E} and e_{I_F} represent the energy costs per unit of immune component I_E and I_F. Their values were assumed to be constant among individuals.

In the EB equation, E_{intake} was obtained using individual spline estimate of FI according to the time of infection and assuming constant feed characteristics:

$$E_{intake} = FI \cdot DMC_{Feed} \cdot MEC_{Feed} \quad \text{Eq. (16)}$$

The energy requirement for protein accretion (E_{growth}) was driven by the temporal changes in carcass protein (P) and $Wool$:

$$E_{growth} = e_{growth} \cdot \left(\frac{dP}{dt} + \frac{dWool}{dt}\right) \quad \text{Eq. (17)}$$

where P followed a Gompertz growth, with a target amount of protein at maturity (P_m) and a growth rate parameter (β_P) estimated individually:

$$\frac{dP}{dt} = \beta_P \cdot \left(\frac{P}{P_m^{\alpha_{P_m}}}\right) \cdot log\left(\frac{P_m}{P}\right) \quad \text{Eq. (18)}$$

$Wool$ was assumed to growth proportionally to P and was depleted when sheep were shorn.

$$\frac{dWool}{dt} = \beta_{Wool} \cdot P \quad \text{Eq. (19)}$$

Finally, the ratio between P and scaled mature protein ($P_m^{\alpha_{P_m}}$) determined the change in energy requirements for animal maintenance during its development:

$$E_{maint} = e_{maint} \cdot \left(\frac{P}{P_m^{\alpha_{P_m}}}\right) \quad \text{Eq. (20)}$$

Based on previous state variables P and L and on estimated FI, observed growth traits (BW and BFT) were defined as auxiliary variables with fixed parameters (specified in Table 1). Bodyweight was the sum of the different body components:

$$BW = P + L + Wool + Ash + Water + Gut\_Fill \quad \text{Eq. (21)}$$

with

$$Ash = \gamma_{Ash} \cdot P \quad \text{Eq. (22)}$$

$$Water = \gamma_{Water} \cdot P_m \cdot \left(\frac{P}{P_m}\right)^{\alpha_{Water}} \quad \text{Eq. (23)}$$

and

$$Gut\_Fill = FI \cdot \left(a_{Gut\_Fill} - b_{Gut\_Fill} \cdot MEC_{Feed}\right) \quad \text{Eq. (24)}$$

Back fat thickness was derived from a previous allometric equation (Macfarlane et al., 2006), as follows:

$$BFT = exp\left(\frac{log(L) - a_{BFT} - b_{BFT} \cdot log(BW - Gut\_Fill)}{c_{BFT}}\right) \quad \text{Eq. (25)}$$

3.2 Experimental data from task 3.2

We used data from task 3.2 describing an artificial infestation experiment in growing female lambs from two lines divergently selected for resistance to *H. contortus* (referred to as "Parasite resistance ROMANE sheep lines" in D3.2). Both lines originated from a prolific meat sheep breed (Romane) bred indoor at INRAE experimental facilities. Sheep were selected for resistance to parasites based on FEC measures, following a unique protocol comprising two successive infections as outlined in detail in (Sallé et al., 2012). Briefly, in the initial population, 274 naïve lambs were infected with a single dose of 10,000 L3 of *H. contortus* to stimulate a primary immune response; 4 weeks later they were treated (0.2 mg/kg of live weight of ivermectin; Oramec, Boerhinger Ingelheim, Lyon, France); after 2 weeks of recovery they were re-infected with a single dose of 10,000 L3 to simulate a secondary immune response and finally treated 5 weeks later. At the end of first and second infection, FEC was recorded just before treatment and those measures were combined to estimate animal breeding values for resistance used as selection criterion to generate the two divergently selected lines.

This study then used data from ewe lambs from the second generation of selection for resistance (R = low FEC) or susceptibility (S = high FEC). At G2, the divergence in FEC between R and S sheep reached 1.9 phenotypic SD (σp) and 3.8 genetic SD (σg) calculated from the initial population (G0). Specifically, 91 female lambs were infected early to stimulate a primary immune response, and again at 4 months of age, following the same infection protocol as described above, except that the first dose was of 3,500 L3/sheep to limit the potential negative consequences of infection on fertility at first mating (at 8–9 months of age). The longitudinal data collected during the second infection were then used in this study to calibrate the host-parasite interaction model. Data included voluntary concentrate intake (in

kg/d; measured daily with automatic feeders) and five other traits measured at day 0, 17, 24, 28, 31, and 35 post-infection: FEC (in egg/g; measured by the modified McMaster technique), blood haematocrit (in %; measured by microhaematocrit centrifugation technique), body weight (in kg), back fat thickness and muscle thickness (BFT and MT, in mm; measured by ultrasound scan on both sides at the 12th– 13th lumbar vertebra (Easi- Scan™, IMV imaging)). Those traits could be linked to the model as shown in Fig.1. E_{intake} was estimated from concentrate intake and diet characteristics (Table 1) assuming that concentrate was the main source of feed energy (i.e. straw intake was considered as negligible).

3.3 Methodology for parameter estimation

According to the model, observed differences in the above measurable performance and resistance traits are caused by individual differences in the genetic potentials for growth (protein and lipid deposition) and wool production, as well as in the immune-response. These can be represented by the model parameters $\theta = (P_m, L_m, \beta_P, \beta_{Wool}, \varphi_{I_E}, \varphi_{I_F})$, (Table 1). In particular, sheep from the two selection lines for resistance described above would be expected to differ in the immune parameters (φ_{I_E}, φ_{I_F}), but possibly not in their growth or wool production parameters as selection was on resistance only. To account for individual variation in these latent parameters, these parameter values associated with each individual were estimated from the data, together with the constant population-specific energy costs (e_{I_E} and e_{I_F}) associated with one unit of I_E and I_F respectively, in two main steps (Figure 3).

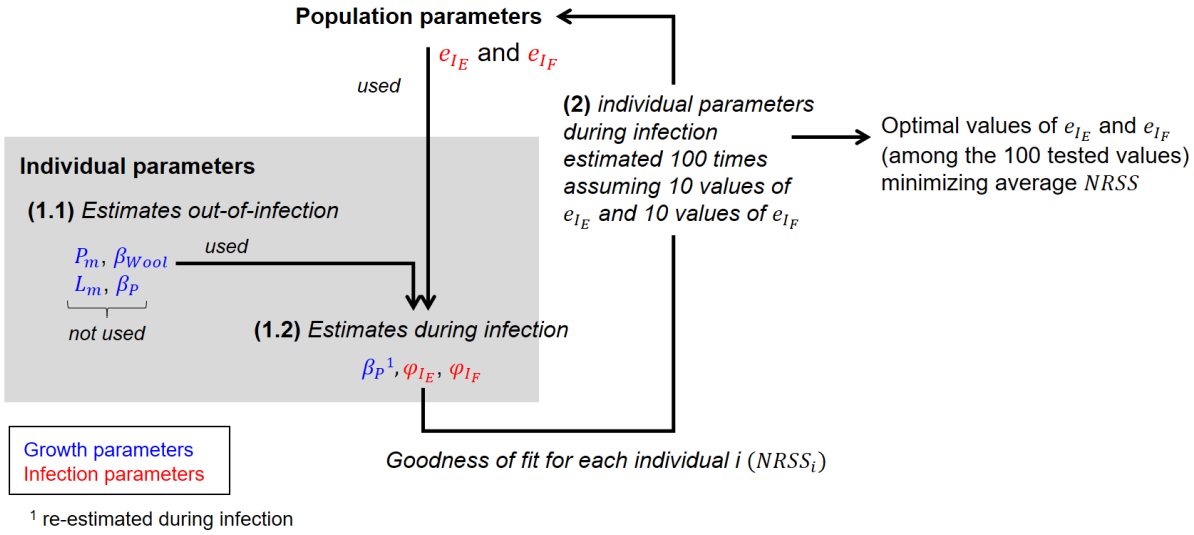

***Figure 3**: Workflow of the model parameter estimation. Grey box indicates the two steps (1.1 and 1.2) of individual parameter estimation. Step (2) iterates the process 100 times to determine the optimal values of energy costs of immunity against* H. contortus *infection.*

First, estimates for the individual parameters $\theta = (P_m, L_m, \beta_P, \beta_{Wool}, \varphi_{I_E}, \varphi_{I_F})$ were obtained. One part of those individual parameters related to growth ($P_m, L_m, \beta_P, \beta_{Wool}$) were estimated using data out-of-infection to describe the growth potential of each individual (step 1.1 in Figure 3). The other individual parameters that were related to immunity ($\varphi_{I_E}, \varphi_{I_F}$) were estimated using data during the infection period. For this last part, we assumed that values of growth parameters related to protein growth (P_m, β_{Wool}) were the same as out of infection, except the rate of protein synthesis β_P that may be affected by infection and was thus re-estimated simultaneously to φ_{I_E} and φ_{I_F} (step 1.2 in Figure 3). When estimating the three parameters during the infection stage, we assumed fixed

constant values of the immune energy costs (e_{I_E} and e_{I_F}) and other population specific parameters listed in Table 1. Individual parameter estimates were obtained by minimizing differences between model predictions and data for that individual as outlined below. This procedure was then repeated for 100 different combinations of values for e_{I_E} and e_{I_F}, and the most likely values of e_{I_E} and e_{I_F} were then selected as those that that minimise the differences between model predictions and data across all individuals (step 2 in Figure 3).

3.3.1 Fitting criteria

Individual values for the parameters were estimated based on the minimization of a normalized residual sum of squares for each individual *i* ($NRSS_i$) defined as follows:

$$NRSS_i = \sum_{k=1}^{K} \left(\frac{\sum_{t=1}^{T_k} \left(\hat{y}_{k,t,i} - y_{k,t,i} \right)^2}{SD(y_{k,i})} \right) \quad \text{Eq. (26)}$$

where $y_{k,t,i}$ and $\hat{y}_{k,t,i}$ are the observed and predicted values, respectively, of trait k for individual i at time t. T_k is the last time-measurement for trait k, K is the number of measured traits and $SD(y_{k,i})$ is the standard deviation of trait k for individual i that is used to normalize each $RSS_{k,i}$. Note that each time-specific measurement of trait k is given the same weight when calculating the whole $NRSS_i$. When $SD(y_{k,i})$ = 0 (as it can be the case for FEC (log-transformed)) it was replaced by 1.

The predicted values $\hat{y}_{k,t,i}$ were obtained using the host-parasite model with a given set of parameters θ. We searched for the set of parameters θ^* that minimize $NRSS_i$ using a modified version of the Levenberg-Marquardt algorithm. This was implemented in R using the *nls.lm* function of the R-package *minpack.lm*.

The exact approach associated with the different steps is outlined below.

3.3.2 Estimation of individuals' growth parameters out-of-infection (step 1.1)

In this step 1.1 (Figure 3), K = 3 traits ($BW, BFT\ and\ Wool$) were used to determine the values of the four parameters $\theta^* = (P_m,\ L_m,\ \beta_P,\ \beta_{Wool})$ that minimise the corresponding $NRSS_i$. A mentioned earlier, a central model assumption was that growth was driven by protein accretion to reach a genetically determined target value at maturity P_m. However this value could not be estimated reliably during the infection as the corresponding growth period was relatively short and feeding conditions were very favourable to fattening (i.e. concentrate *ad libitum*) compared to the periods where animals were uninfected (forage and concentrate to meet animal requirements). In this first step we thus aimed to estimate P_m using growth data before and after the experimental period to capture the 'normal' growth pattern before reproduction (Fig. 4A). For this we used the empirical growth equation (Eq. (18)). In addition to P_m we also estimated the 'normal' protein growth rate parameter β_P even though we considered that this parameter could vary during infection (cf. next sub-section 3.2.4). Based on BFT and $Wool$ measurements it was possible to separate P_m from other BW components at maturity (following Eq. (21-25)). Data on BFT (Fig. 3B) was informative of the level of lipid. However, as food intake was not recorded out of the infection lipid deposition could not be calculated based on EB during those periods (as shown in Eq. (14)). Instead a 'normal' lipid growth was assumed to follow a sigmoid pattern as proposed in (Emmans, 1997). This pattern is driven by $\frac{dP}{dt}$ as follows:

$$\frac{dL}{dt} = \frac{dP}{dt} \cdot \frac{L_m}{P_m} \cdot d \cdot \left(\frac{P}{P_m}\right)^{d-1} \quad \text{Eq. (27)}$$

where the estimated parameter L_m represents the level of L at maturity.

Based on fleece weight recorded after the experimental period (Fig. 3A), we could also estimate the individual wool growth parameter β_{Wool} of Eq. (19). Finally, in Eq. (21) all other BW components than P, L and $Wool$ were simply derived from P, assuming equal parameter values among individuals.

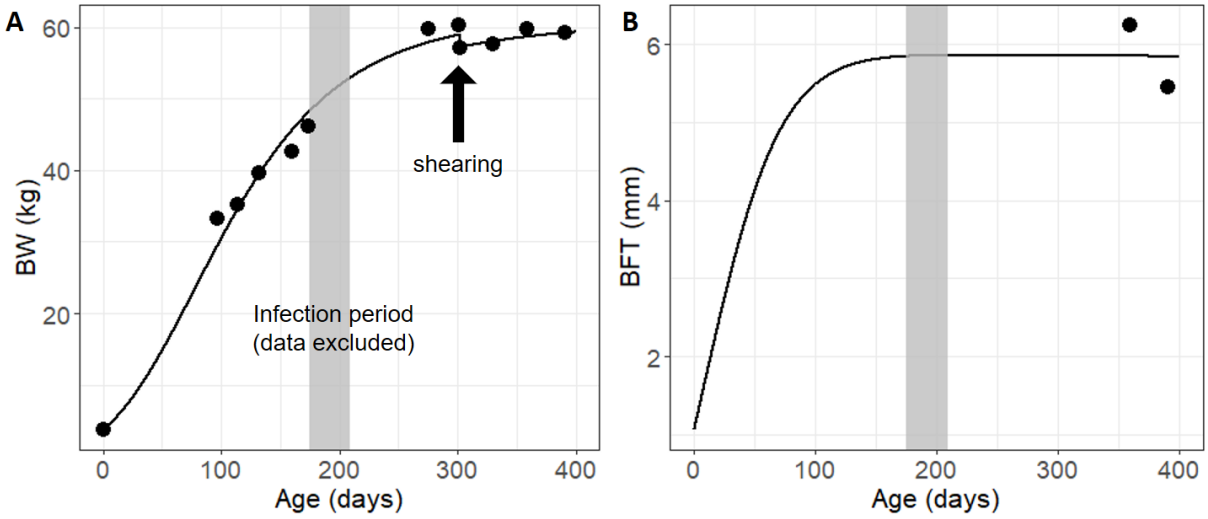

***Figure 4**: Example of individual growth curve fitting to estimate protein weight at maturity based on body weight (BW) (**A**) and back fat thickness (BFT) (**B**) data measured out of infection. Points and solid lines represent observed data and model predictions, respectively.*

3.3.3 Estimation of individuals 'parameters during infection for fixed values of immune energy costs (step 1.2)

During the infection we used the two coupled sub-models (i.e. the host-parasite system and the host energy balance). Individually we estimated parameters φ_{I_E} and φ_{I_F} that set the magnitude of the two immune responses. For the energy balance sub-model, we used the values of P_m and β_{Wool} estimated out-of- infection (see previous sub-section) whereas we re-estimated β_P considering that the protein growth rate (but not the target P_m) could deviate from the normal value estimated out-of-infection. In this step 1.2 (Fig. 3), lipid deposition was calculated based on food intake (Eq. (14)) so the parameter L_m was no longer needed. All other parameters related to immune responses were assumed equal among-individuals, including e_{I_E} and e_{I_F}. Thus, for each individual *i* the values of the parameters (φ_{I_E}, φ_{I_F} and β_P), were determined that minimise the individual's $NRSS_i$ comprising K = 4 traits (FEC, HE, BW, BFT).

3.3.4 Estimating the immune energy costs e_{I_E} and e_{I_F} (step 2)

Estimates of individuals' immune parameters following the procedure outlined in 3.3.1 were obtained for 100 (10 × 10) different combinations of values of e_{I_E} and e_{I_F} (step 2; Fig. 3). These combinations comprised 10 different values of e_{I_E} and e_{I_F}, respectively (within the range [0 ; 0.03] and [0 ; 0.021] ; for e_{I_E} and e_{I_F} respectively, with 10 equal increments within each case). For each combination, *NRSS* calculated during the infection (with K = 4 traits) was averaged over all individuals (from both lines).

The most likely combination of e_{I_E} and e_{I_F} was then considered as the one that minimize the average $NRSS$.

3.3.5 Predicted resilience trajectories

To illustrate the different effects investigated in terms of dynamic individual responses over the course of the infection we represented the trajectories of the four observed traits (FEC, HE, BFT and BW) using the parameters corresponding to the different scenario.

To assess the effect of positive immune energy costs, resilience trajectories were predicted for the scenario corresponding to the observed situation (using the optimal immune energy costs) vs. a scenario of zero energy cost (e_{I_E} = 0 and e_{I_F} = 0) .

To assess the effect of a nutritional challenge, resilience trajectories were also predicted for a scenario where the energy content of the feed intake was reduced compared to the observed situation.

4 Results

4.1 Growth parameters out-of-infection

No difference was observed between the two selection lines among the four growth parameters estimated out of infection (Table 2). Note that the values of β_P were close to the interspecific estimate (sheep and cattle) found by (Emmans, 1997) and equal to 0.02335 (termed 'B*' in (Emmans, 1997)).

***Table 1**: Mean (with standard deviation) of growth parameters estimated out of infection in sheep from lines selected on resistance (R) or susceptibility (S) to* Haemonchus contortus*. Parameters are defined in Table 1. Line differences were tested based on unpaired t-test.*

Parameter	Line R (n = 21)	Line S (n = 21)	t (df = 40)	p
P_m	6.88 (0.364)	6.75 (0.433)	1.027	0.31
L_m	15.08 (2.033)	15.55 (2.602)	-0.641	0.53
β_P	0.0224 (0.0025)	0.0239 (0.0037)	-1.551	0.13
β_{Wool}	$11 \cdot 10^{-5}$ ($3.5 \cdot 10^{-5}$)	12.10^{-5} ($2.7 \cdot 10^{-5}$)	-0.518	0.61

4.2 Energy costs of resistance to *H. contortus* ($e_{I_E}$and e_{I_F})

Across the 42 individuals, the best average model fit was found for two positive value among the two energy costs assumed for immunity (i.e. e_{I_E} = 0.01 and e_{I_F} = 0.0072; Fig. 5).

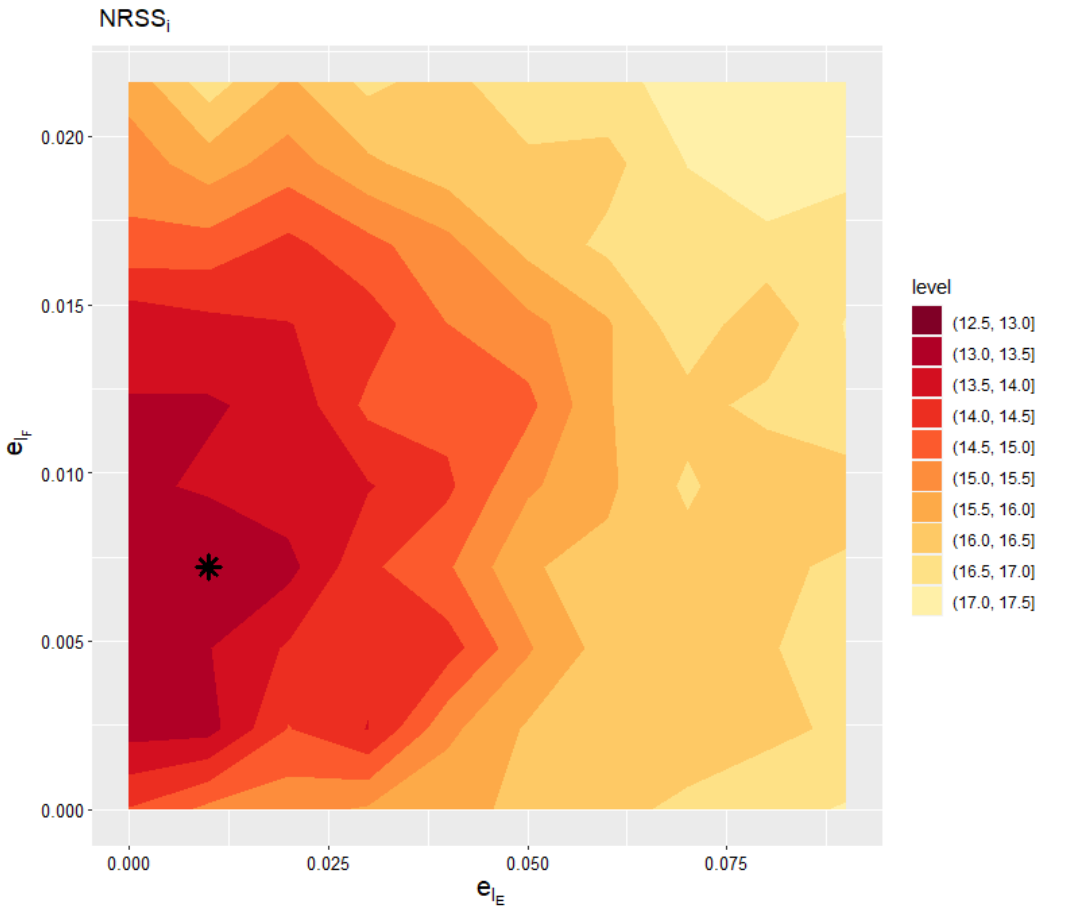

Figure 5: *Model goodness of fit according to the assumed values for the energy cost of immunity against* H. contortus *(e_{I_E} and e_{I_F} controlling immunity against larvae establishment and fecundity, respectively). The fitting criteria used for parameter estimation was the normalized residual sum of squares for each individual* i *($NRSS_i$). The average $NRSS$ over the 42 individuals is represented. The global optimum is indicated with an asterisk.*

Assuming immune energy costs improved the goodness-of-fit (mean of $NRSS_i$ = 12.97 (SD = 4.73)) compared to the scenario where no immune energy cost was assumed ($NRSS_i$ = 14.54 (7.04)). This improvement was mostly observed in the R line. Indeed, under the zero-energy cost assumption the model tended to overestimate BW and BFT in the R line in particular, whereas this energy excess could be partly accounted for by the higher resistance to parasites in this line compared to the S line.

The immune energy cost assumption affected the three individual parameters estimated during the infection (i.e. $\varphi_{I_E}$and φ_{I_F} related to immunity and β_P related to growth). As expected higher values of $\varphi_{I_E}$and φ_{I_F} were observed in the R line compared with the S line, regardless of whether energy costs apply or not. However assuming a positive energy cost further constrained the optimisation process which slightly attenuated the difference between lines (Table 3). In contrast, when immune energy costs applied, estimates of β_P became closer and similar between lines. In general those estimates of β_P were lower during the infection period (c.a. 0.014-0.018) than out of infection (c.a. 0.023; Table 2).

***Table 2**: Mean values of immunity and growth parameters estimated during infection in sheep from lines selected on resistance (R) or susceptibility (S) to* Haemonchus contortus*. Parameters are defined in Table 1. Lines differences were tested based on unpaired t-test.*

	Zero immune energy cost (e_{I_E} = 0 and e_{I_F} = 0)				Optimal immune energy costs (e_{I_E} = 0 and e_{I_F} = 0.0048)			
Parameter	Line R (n = 21)	Line S (n = 21)	t (df = 40)	p	Line R (n = 21)	Line S (n = 21)	t (df = 40)	p
φ_{I_E}	1.336	0.950	2.44	0.019	1.184	0.967	3.95	0.001
φ_{I_F}	-5.291	-7.369	4.56	< 0.001	-5.114	-7.294	4.74	< 0.001
β_P	0.0185	0.0154	1.4	0.17	0.0141	0.0143	-0.104	0.92

[a] re-estimated during infection

4.3 Predicted resilience trajectories to the infectious challenge

Individual model fits corresponding to the energy costs estimates for parasite resistance identified through the optimisation process above were relatively good as shown with two representative individuals of each line ($NRSS$ = 13.9 and 14.6) (Fig. 6). The consequences of the positive energy costs for parasite resistance were observed in terms of a reduction of BW and BFT gains compared to the predicted trajectories if parasite resistance was costless (Fig.6).

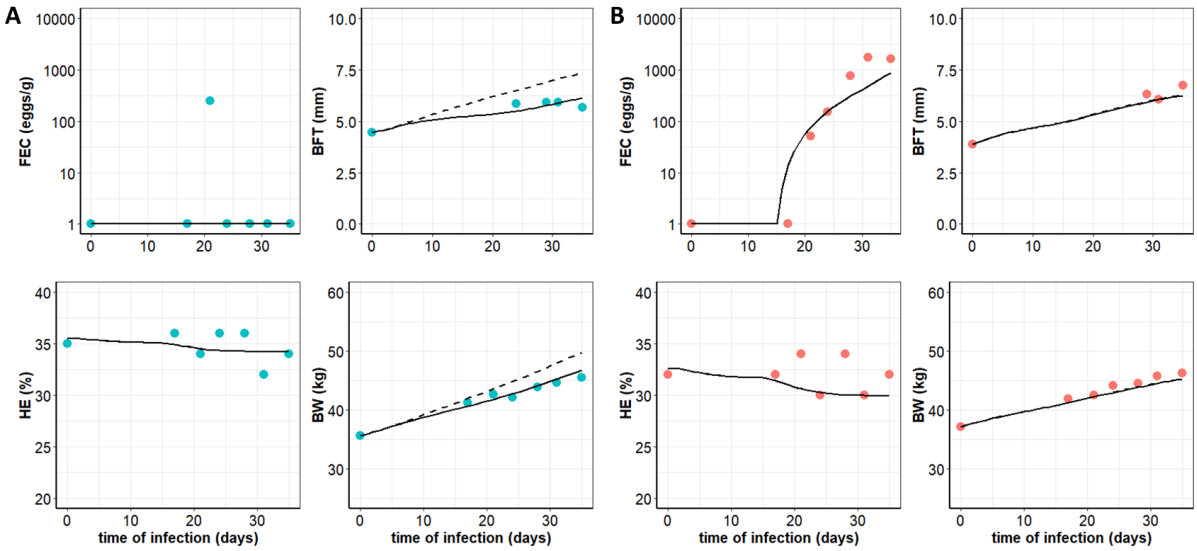

*Figure 6: Predicted resilience trajectories for two representative sheep of lines selected for parasite resistance (**A**) or susceptibility (**B**) according to the energy cost assumed for parasite resistance. Points represent observed data, solid lines are model predictions for the optimum energy costs assumed (i.e. e_{I_E} = 0.01 and e_{I_F} = 0.0072), dashed lines are model predictions when no energy costs for parasite resistance are assumed (i.e. e_{I_E} = 0 and e_{I_F} = 0). FEC = fecal parasite egg count; HE = blood haematocrit; BFT = backfat thickness; BW = body weight.*

4.4 Trade-off between parasite resistance and fat deposition

The immune energy costs and of the higher immune response in the R line compared to the S line could partly explain the difference observed between lines in terms of BFT during the infection (Fig. 7A). This difference was associated with a relative energy allocation to immunity that was about three

times larger the R line compared to the S line on average (Fig. 7B). As a result, a trade-off was predicted between BFT gain and parasite resistance (Fig. 7C) as supported by the positive correlation between those traits (pearson r = +0.40, $t_{(40)}$ = 2.80, p = 0.008).

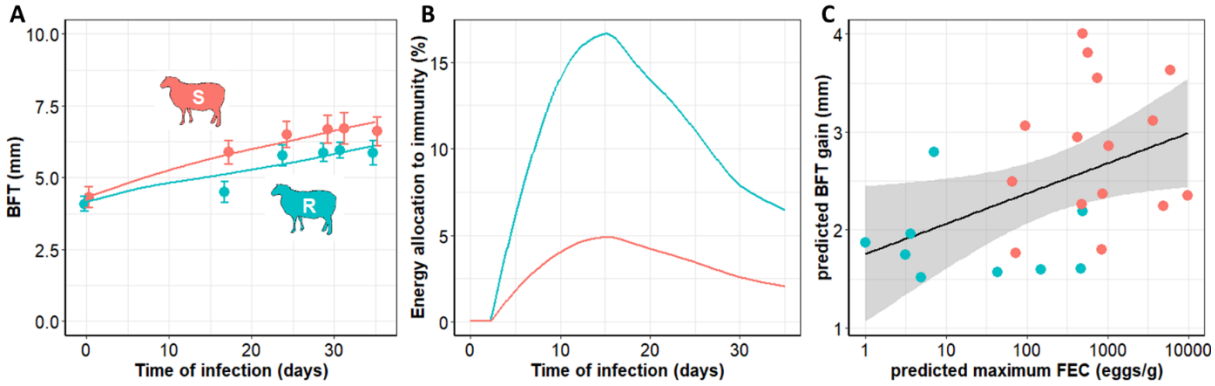

***Figure 7**: Average observed and predicted back fat thickness (BFT) (**A**), predicted energy allocation to immunity (**B**) and predicted BFT gain and maximum parasite fecal egg count (FEC) (**C**) during an infectious challenge with* Haemonchus contortus *in sheep line selected on resistance (R) or susceptibility (S) to the parasite. Average model fit (solid line) within each sheep line are represented, together with observations (points = means; error bars = 95% confidence interval) for BFT. Relative energy allocation to immunity was defined as the proportion of energy intake allocated to immunity against* H. contortus*. Predicted BFT gains were calculated between the start (day 0) and the end (day 35) of the infectious challenge. The solid line and the grey area in (C) represents the linear regression line (predicted BFT = 1.98 + 0.087 · predicted max FEC) with the prediction interval.*

4.5 Trade-offs and resilience trajectories under a supplementary nutritional challenge

To explore the model sensitivity to different feeding conditions, individual resilience trajectories to infectious challenge were simulated for the same feed intake but assuming a range of different values for the feed energy content. For each individual the absolute energy allocation to immunity against *H. contortus* was assumed to be maintained across the different feeding conditions while the potential energy deficit or excess were managed through body lipid mobilisation or deposition, respectively. As a result, the trade-off between parasite resistance and fat deposition was stronger when energy intake decreased as shown by higher values of the correlations between the maximum FEC and BFT gain, and to a lesser extent between HE loss and BFT gain (Fig. 8). In contrast, the correlation between BW gain and maximum FEC or HE loss remained close to zero.

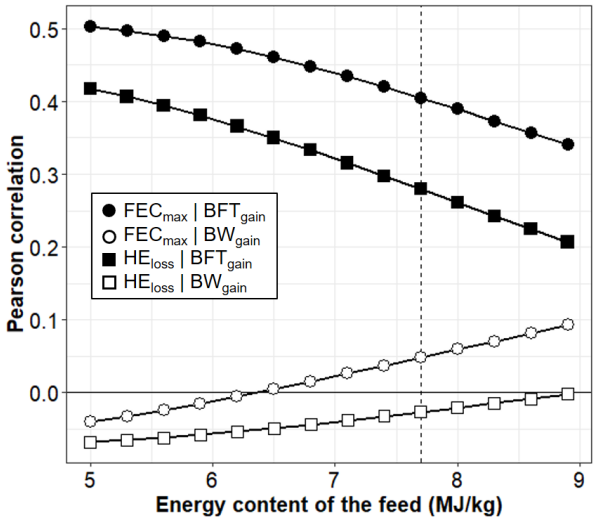

Figure 8: *Environmental sensitivity of the correlations between two health traits and two growth traits calculated from the host-parasite model. Environmental variation was simulated through a variation of the energy content of the feed intake. Vertical dashed line indicates the feed energy content estimated in the experiment. Individual traits were derived from simulations of the same infectious challenge as described in the experiment. Health traits included maximum fecal egg count (FEC_{max}) and loss of blood haematocrit (HE_{loss}). Growth traits included gains in back fat thickness (BFT_{gain}) and in body weight (BW_{gain}).*

The effect of a nutritional challenge on the predicted resilience trajectories is illustrated in Fig. 9 for the two representative individuals of each line previously reported (Fig. 6). The nutritional challenge corresponds to a reduction of the energy content of the diet of about 15% the level assumed in the experiment (from 7.7 to 6.5 MJ/kg of DM). The effect of this challenge was mainly observed as a reduced gain in BFT, whose absolute magnitude was on average not different between lines (- 0.85 mm between the start and the end of infectious period). However as BFT gain was lower in the R line with the experimental diet (Figure 7A), the nutritional challenge was predicted to be relatively stronger on average in this line (- 44%) than in the S line (-33%). As indicated by the previous correlations (Fig, 8), a negligible of the nutritional challenge on BW was predicted. This partly resulted from the different effects on the various components of BW. In Fig. 9, note that BW was slightly higher at the start of the infectious challenge as gut fill was predicted to be higher when the energy content decreases (see Eq. 24). This higher gut fill was then compensated by the lower lipid mass.

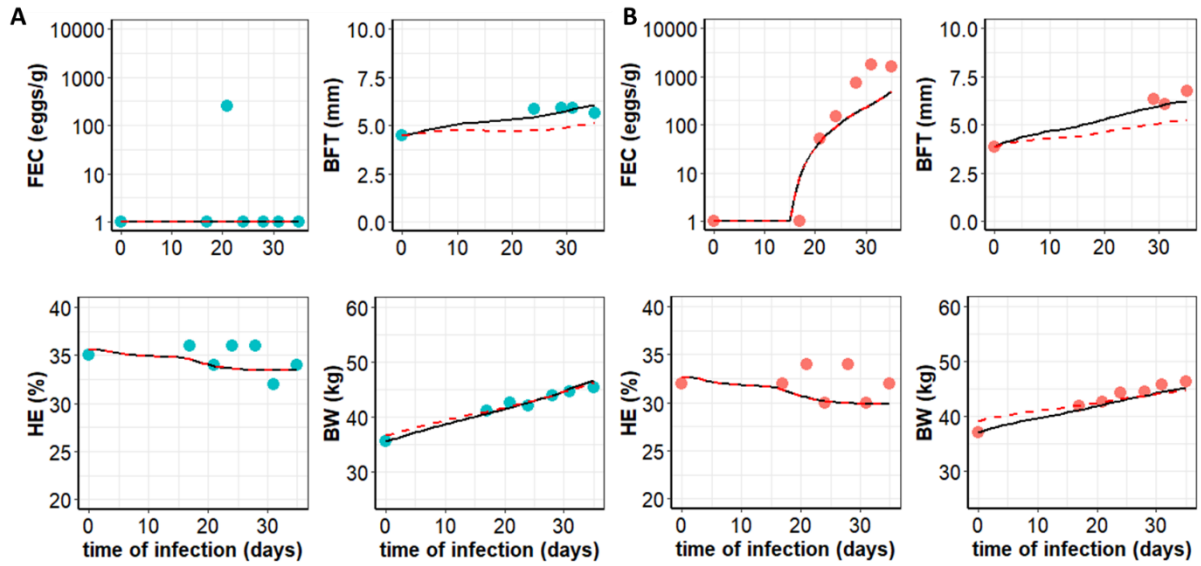

*Figure 9: Predicted resilience trajectories for two representative sheep of lines selected for parasite resistance (**A**) or susceptibility (**B**) according to the diet energy density. Points represent observed data, solid lines are model predictions for the assumed energy content of the experimental diet (7.7 MJ/kg of DM), red dashed lines are model predictions when a lower energy content is assumed (6.5 MJ/kg of DM). FEC = faecal parasite egg count; HE = blood haematocrit; BFT = backfat thickness; BW = body weight. Both scenarios were simulated assuming the optimum energy costs for parasite resistance.*

5 Discussion

Although previous mechanistic models of gastro-intestinal parasite infection in sheep assumed a nutritional cost of parasite resistance (Vagenas et al., 2007b; Doeschl-Wilson et al., 2008; Laurenson et al., 2011; Saccareau et al., 2016), the magnitude of such cost remains hypothetical and challenging to estimate from real data. Studies in nutrition have focused on the nutritional costs of infection due for instance to host resources consumption by parasites and on the negative consequences on productive traits (e.g. Ceï et al., 2018). In terms of economic impacts on farm, the costs of parasite infections are also emphasized compared with the costs of parasite resistance (Mavrot et al., 2015). Yet the existence of parasite resistance costs is supported both by the theory (Sheldon and Verhulst, 1996) and by experimental evidence (Lochmiller and Deerenberg, 2000; Greer, 2008). Those costs are not only important from a nutritional viewpoint but also from a genetic viewpoint as they may constrain the functional relationship between traits and thereby underlay unfavourable genetic correlations between parasite resistance and production traits (Bishop and Stear, 2003). Our study is to our knowledge the first attempt to quantify dynamically such resistance costs in the case of gastro-intestinal parasite infection in sheep.

Based on our model and on experimental data, the energy costs of resisting to *H. contortus* infection could be at the basis of a trade-off between parasite resistance and fat deposition in growing lambs. Although some data support a potential antagonism between parasite resistance and body growth (e.g. a positive correlation between FEC and BW; Mucha et al. (2022)), few have investigated the changes in body composition during parasite infection. In general, nutritional costs are assumed in terms of metabolisable protein (Bishop and Stear, 1997; Liu et al., 2005; Vagenas et al., 2007b) which should primarily lead to consequences on body muscle rather than body fat dynamics. However there is evidence for energy costs of parasite resistance in genetically resistant sheep (Liu et al., 2005). Those

costs will be more likely revealed when feed energy is very limiting compared with feed protein, as was the case in our experiment. Still, repeating the same infection protocol than in our experiment but using different diets (i.e. various protein and energy contents) would be needed to go further into the nature of parasite resistance costs.

Besides the uncertainty that arose from the single dataset that we used to calibrate our model, some model assumptions are important to remind to interpret the significance of the estimated parasite resistance costs. In particular, we assumed that host energy balance was fully buffered with body reserves. This may not necessarily occur as animals may also defend a certain level of body fat and therefore adjust their energy allocation for instance between protein growth and immunity. As assumed by Coop and Kyriazakis (1999) protein growth and immunity were given the higher priority compared with changes in body lipid in our model. Yet more complex allocation rules could be assumed (e.g. Sandberg et al., 2005), which may notably lead to different trade-off expressions according to the diet energy content (compared with our predictions in Fig. 8). Here our model results fit the predictions of the resource allocation theory (Doeschl-Wilson et al., 2009) and thus provide a first step towards a prediction tool that could be used in practice. Our model focuses on short infection challenge with a single parasite specie and under specific controlled indoor conditions. Further model developments are thus clearly needed to predict trade-offs in the context of parasite infections naturally occurring on farm pastures (e.g. multiple infections, other host sex or stages, costs of parasite infection). As it was presented here, the model represent a first tool to assist breeding strategies since the infection protocol that has been modelled here has proven to be effective to select genetically resistant rams (Aguerre et al., 2018).

6 Conclusion

This document outlines the scope, assumptions and methodology for a mechanistic resource allocation model of host-parasite infections in sheep. Resilience trajectories were generated for an infectious challenge under controlled conditions. Further the effect of a nutritional challenge superimposed to the infectious challenge could be explored by simulating resilience trajectories using a reduced energy content of the diet. The model has been calibrated with data generated in task 3.2 of SMARTER in lambs of the parasite resistance Romane sheep lines. This allowed the estimation of a key unknown model parameter that underpins trade-offs generated by immune or nutritional challenges: the energy cost of parasite resistance. The study provided the first empirical evidence for a positive energy cost associated with host resistance to parasites. This energy cost can lead to a genetic trade-off between parasite resistance and fat deposition in lambs and may thus constrain breeding strategies in particular when feed energy is scarce.

The estimation of this energy cost of parasite resistance allows model predictions of host response and resilience trajectories under different parasitic or nutritional challenges, as demonstrated in this study.

To determine trade-off under nutitional challenge, a second resource allocation model has been developped in SMARTER. Data from the longevity goat experiment were used to infer mean trajectories for milk production and body weight. Links between the performance trajectories and the resilience of these animals to a short-term nutritional challenge have been explored and used, together with other literature data. Once it has been calibrated with those data, the goat allocation-acquisition model (AQAL-Goat) can predict life-time trajectories of intake (DM and energy) and body

components, such as mass, fat, protein, and energy. This preliminary work is described in Appendix2.

7 Deviations or delays

N/A

8 References

Aguerre, S., P. Jacquiet, H. Brodier, J. P. Bournazel, C. Grisez, F. Prévot, L. Michot, F. Fidelle, J. M. Astruc, and C. R. Moreno. 2018. Resistance to gastrointestinal nematodes in dairy sheep: Genetic variability and relevance of artificial infection of nucleus rams to select for resistant ewes on farms. Veterinary Parasitology. 256:16–23. doi:10.1016/j.vetpar.2018.04.004.

Beilharz, R. G., B. G. Luxford, and J. L. Wilkinson. 1993. Quantitative genetics and evolution: Is our understanding of genetics sufficient to explain evolution? Journal of Animal Breeding and Genetics. 110:161–170. doi:10.1111/j.1439-0388.1993.tb00728.x.

Bishop, S. C., and M. J. Stear. 1997. Modelling responses to selection for resistance to gastro-intestinal parasites in sheep. Animal Science. 469–478.

Bishop, S. C., and M. J. Stear. 2003. Modeling of host genetics and resistance to infectious diseases: understanding and controlling nematode infections. Veterinary Parasitology. 115:147–166. doi:10.1016/S0304-4017(03)00204-8.

Ceï, W., N. Salah, G. Alexandre, J. C. Bambou, and H. Archimède. 2018. Impact of energy and protein on the gastro-intestinal parasitism of small ruminants: A meta-analysis. Livestock Science. 212:34–44. doi:10.1016/j.livsci.2018.03.015.

Colditz, I. G. 2007. Six costs of immunity to gastrointestinal nematode infections. Parasite Immunol. 0:071025012052001-??? doi:10.1111/j.1365-3024.2007.00964.x.

Coop, R. L., and I. Kyriazakis. 1999. Nutrition–parasite interaction. Veterinary Parasitology. 84:187–204. doi:10.1016/S0304-4017(99)00070-9.

Dargie, J. D., and E. W. Allonby. 1975. Pathophysiology of single and challenge infections of Haemonchus contortus in Merino sheep: Studies on red cell kinetics and the “self-cure” phenomenon. International Journal for Parasitology. 5:147–157. doi:10.1016/0020-7519(75)90021-1.

Doeschl-Wilson, A. B., W. Brindle, G. Emmans, and I. Kyriazakis. 2009. Unravelling the Relationship between Animal Growth and Immune Response during Micro-Parasitic Infections. S. Plaistow, editor. PLoS ONE. 4:e7508. doi:10.1371/journal.pone.0007508.

Doeschl-Wilson, A. B., D. Vagenas, I. Kyriazakis, and S. C. Bishop. 2008. Exploring the assumptions underlying genetic variation in host nematode resistance *(Open Access publication)*. Genet. Sel. Evol. 40:241–264. doi:10.1051/gse:2008001.

Emmans, G. C. 1997. A Method to Predict the Food Intake of Domestic Animals from Birth to Maturity as a Function of Time. Journal of Theoretical Biology. 186:189–199.

Fenton, A., and S. E. Perkins. 2010. Applying predator-prey theory to modelling immune-mediated, within-host interspecific parasite interactions. Parasitology. 137:1027–1038. doi:10.1017/S0031182009991788.

Greer, A. W. 2008. Trade-offs and benefits: implications of promoting a strong immunity to gastrointestinal parasites in sheep: Trade-offs and benefits of immunity. Parasite Immunology. 30:123–132. doi:10.1111/j.1365-3024.2008.00998.x.

Kahn, L. P., M. R. Knox, G. D. Gray, J. M. Lea, and S. W. Walkden-Brown. 2003. Enhancing immunity to nematode parasites in single-bearing Merino ewes through nutrition and genetic selection. Veterinary Parasitology. 112:211–225. doi:10.1016/S0304-4017(02)00438-7.

Laurenson, Y. C. S. M., S. C. Bishop, and I. Kyriazakis. 2011. *In silico* exploration of the mechanisms that underlie parasite-induced anorexia in sheep. Br J Nutr. 106:1023–1039. doi:10.1017/S0007114511001371.

Laurenson, Y. C. S. M., I. Kyriazakis, and S. C. Bishop. 2012. In silico exploration of the impact of pasture larvae contamination and anthelmintic treatment on genetic parameter estimates for parasite resistance in grazing sheep1. Journal of Animal Science. 90:2167–2180. doi:10.2527/jas.2011-4527.

Liu, S. M., T. L. Smith, L. J. E. Karlsson, D. G. Palmer, and R. B. Besier. 2005. The costs for protein and energy requirements by nematode infection and resistance in Merino sheep. Livestock Production Science. 97:131–139. doi:10.1016/j.livprodsci.2005.03.007.

Lochmiller, R. L., and C. Deerenberg. 2000. Trade-offs in evolutionary immunology: just what is the cost of immunity? Oikos. 88:87–98. doi:10.1034/j.1600-0706.2000.880110.x.

Louie, K., A. Vlassoff, and A. Mackay. 2005. Nematode parasites of sheep: Extension of a simple model to include host variability. Parasitology. 130:437–446. doi:10.1017/S003118200400678X.

Macfarlane, J. M., R. M. Lewis, G. C. Emmans, M. J. Young, and G. Simm. 2006. Predicting carcass composition of terminal sire sheep using X-ray computed tomography. Anim. Sci. 82:289–300. doi:10.1079/ASC200647.

Mavrot, F., H. Hertzberg, and P. Torgerson. 2015. Effect of gastro-intestinal nematode infection on sheep performance: a systematic review and meta-analysis. Parasites Vectors. 8:557. doi:10.1186/s13071-015-1164-z.

Mucha, S., F. Tortereau, A. Doeschl-Wilson, R. Rupp, and J. Conington. 2022. Animal Board Invited Review: Meta-analysis of genetic parameters for resilience and efficiency traits in goats and sheep. animal. 16:100456. doi:10.1016/j.animal.2022.100456.

Rauw, W. M., ed. 2009. Resource allocation theory applied to farm animal production. 1st ed. CABI, UK. Available from: http://www.cabidigitallibrary.org/doi/book/10.1079/9781845933944.0000

Saccareau, M., C. R. Moreno, I. Kyriazakis, R. Faivre, and S. C. Bishop. 2016. Modelling gastrointestinal parasitism infection in a sheep flock over two reproductive seasons: *in silico* exploration and sensitivity analysis. Parasitology. 143:1509–1531. doi:10.1017/S0031182016000871.

Saccareau, M., G. Sallé, C. Robert-Granié, T. Duchemin, P. Jacquiet, A. Blanchard, J. Cabaret, and C. R. Moreno. 2017. Meta-analysis of the parasitic phase traits of Haemonchus contortus infection in sheep. Parasites Vectors. 10:201. doi:10.1186/s13071-017-2131-7.

Sallé, G., P. Jacquiet, L. Gruner, J. Cortet, C. Sauvé, F. Prévot, C. Grisez, J.-P. Bergeaud, L. Schibler, A. Tircazes, D. François, C. Pery, F. Bouvier, J.-C. Thouly, J.-C. Brunel, A. Legarra, J. M. Elsen, J. Bouix, R. Rupp, and C. Moreno-Romieux. 2012. A genome scan for QTL affecting resistance to Haemonchus contortus in sheep. Journal of Animal Science. 90:4690–4705. doi:10.2527/jas2012-5121.

Sandberg, F. B., G. C. Emmans, and I. Kyriazakis. 2005. Partitioning of limiting protein and energy in the growing pig: description of the problem, possible rules and their qualitative evaluation. Br J Nutr. 93:205–212. doi:10.1079/BJN20041321.

Sheldon, B. C., and S. Verhulst. 1996. Ecological immunology: costly parasite defences and trade-offs in evolutionary ecology. Trends in Ecology & Evolution. 11:317–321. doi:10.1016/0169-5347(96)10039-2.

Smith, G. 1988. The population biology of the parasitic stages of *Haemonchus contortus*. Parasitology. 96:185–195. doi:10.1017/S0031182000081750.

Stear, M. J., S. C. Bishop, B. A. Mallard, and H. Raadsma. 2001. The sustainability, feasibility and desirability of breeding livestock for disease resistance. Research in Veterinary Science. 71:1–7. doi:10.1053/rvsc.2001.0496.

Vagenas, D., S. C. Bishop, and I. Kyriazakis. 2007a. A model to account for the consequences of host nutrition on the outcome of gastrointestinal parasitism in sheep: model evaluation. Parasitology. 134:1279–1289. doi:10.1017/S0031182007002624.

Vagenas, D., S. C. Bishop, and I. Kyriazakis. 2007b. A model to account for the consequences of host nutrition on the outcome of gastrointestinal parasitism in sheep: logic and concepts. Parasitology. 134:1263–1277. doi:10.1017/S0031182007002570.

Vanimisetti, H. B., S. L. Andrew, A. M. Zajac, and D. R. Notter. 2004. Inheritance of fecal egg count and packed cell volume and their relationship with production traits in sheep infected with Haemonchus contortus1. Journal of Animal Science. 82:1602–1611. doi:10.2527/2004.8261602x.

Wellock, I. J., G. C. Emmans, and I. Kyriazakis. 2004. Modelling the effects of stressors on the performance of poulations of pigs. Jounal of Animal Science. 82:2442–2450.

9 Appendix1: Source code for the sheep allocation model

This is the R code of the infectious model presented in deliverable D3.3 of the SMARTER project. The model was developed with R version 4.2.2 (2022-10-31 ucrt) – "Innocent and Trusting".

The following R packages need to be uploaded first:

```
library(deSolve); library(reshape2); library(minpack.lm)
```

Three components are needed to run a simulation:

- The model function
- The default parameters
- The initial values
-

Model function "InfGrow_model"

```
#################################################################
################ Infection model function  ##################
#################################################################
InfGrow_model <- function(t, state, parameters){
  # t = time
  # state = initial values of state variable
  # parameters = list of constant values used in the model

  with(as.list(c(state, parameters)),{

  # Functional response "funct_rep" later used in the model
    funct_rep <- function(x, x0.5, A = 1, n = 3, inc = TRUE){
      # A = asymptote, n = shape, that is by default 3 (sigmoid) and increasing wi
th input x)
      if(inc==TRUE) x0 <- (x0.5/x)^n else x0 <- (x/x0.5)^n
      return(A/(x0 + 1))}

  # Settings of time delays
    # muLI: mortality rate of ingested larvae before reaching the establishment si
te
    muLI <- -log(E0)/thauLI
    # thauLI = time delay from ingestion to establishment site
    tlag1 <- t - thauLI
    if (tlag1 <= 0) kLE2 <- 0 else kLE2 <- kLE
    tlag2 <- t - thauLE
    #  thauLE = time delay from established larvae LE to adult male (Am) or female
(Af_nl) (i.e. length of L4 stage)
    if (tlag2 <= 0) kA2 <- 0 else kA2 <- kA

  # Food intake and Mass-specific food intake ("Food_intake_prop")
    Food_intake <- predict(interpol, t)$y
    # Food intake is obtained from 'interpol' function which gives an estimate for
each time t
    Food_intake <- Food_intake*(Food_intake>0)
    # Negative estimate replaced by 0
    Food_intake_prop <- as.numeric(c(interpol2$coefficients)%*%c(1,t))
    # Food intake as a proportion to body mass over the period (to calculate gut f
ill)
```

```
  # Immunity effect on parasites (effect of immune components I_E and I_F)
    # E_I is reduction in LI establishment due to immune response I_E (E_I togethe
r with E gives establishment)
    E_I <- funct_rep(x = I_E, x0.5 = I_E0.5, inc = FALSE)
    # kF_I is reduction in Af development due to immune response I_E (kF_I togethe
r with kF0 gives transition rate from Af_nl to Af)
    kF_I <- funct_rep(x = I_F, x0.5 = I_F0.5, inc = FALSE)

  # Parasite transitions between stages LI, LE, Am, Af_nl, Af
    # dLI/dt (LI = ingested larvae)
    dLI <- - muLI*LI - kLE2*LI
    # dLE/dt (LE = larvae established)
    dLE <- E_I*kLE2*LI - muLE*LE - kA2*LE
    # dAm/dt (Am = adult males)
    dAm <-  kA2*sex_ratio*LE - muA*Am
    # dAf_nl/dt (Af_nl = adult females non-laying)
    dAf_nl <-  kA2*(1 - sex_ratio)*LE - muA*Af_nl - kF0*kF_I*Af_nl
    # dAf/dt (Af = adult female laying)
    dAf <-  kF0*kF_I*Af_nl - muA*Af

  # Immune response to parasites
    # dI_E/dt (I_E = immunity against establishment)
    dI_E <-  betaI*(I_E0 - I_E) + rhoI_E*I_E*funct_rep(LI, LI0.5)
    # dI_F/dt (I_F = immunity against adult female laying eggs)
    dI_F <- betaI*(I_F0 - I_F) + rhoI_F*(I_E - I_E0)*LE

  # Sheep growth rates
    # Protein growth
    dProtein <- Protein*(B_Protein/Protein_m^beta_Protein)*log(Protein_m/Protein)
    # Wool growth
    dWool <- K_Wool*Protein
    # Energy balance (= energy available for lipid growth)
    EB <- Food_intake*DM*EEC - (dProtein + dWool)*bp - e_maint*(Protein/Protein_m^
beta_Protein) - (e_IE*I_E + e_IF*I_F)
    # Lipid growth
    dLipid <- (EB/bl)*(EB>=0) + (EB/blc)*(EB<0)

  # Others body components (varying proportionally with Protein mass)
    Ash <- AshtoProtein_ratio*Protein
    Water <- WatertoProtein_ratio*Protein_m*(Protein/Protein_m)^beta_Water
    # Mass-specific gut fill
    Gut_fill_prop <-  Food_intake_prop*(11 - ((7*EEC)/15))
    # Empty body weight
    EBW <- Protein + Lipid + Ash + Water

  # OUTPUTS
    # Body weight
    BW <- (EBW + Wool)/(1 - Gut_fill_prop)
    # Back fat thickness
    fat_thick <- if(Lipid>0) exp((log(Lipid) - bLipid_0 - bLipid_EBW*log(EBW))/bLi
pid_FT) else 0
    # Feces
    Feces <- (1 - dDM)*(Food_intake)*1000

    # Observable host effects
    # dHE/dt (HE = hematocrit)
```

```
    dHE <- betaHE*(HE0 - HE) - kHE_LE*LE - kHE_Anf*(Am + Af_nl) - kHE_Af*Af
    # Egg outputs (FEC = fecal egg count, per gram of feces)
    FEC <- FEC_i*Af/Feces # FEC_i = average daily production of eggs per adult fem
ale

  # (!!order of derivatives needs to be the same as the order state variables (sta
te)!!)
  list(c(dLI, dLE, dAm, dAf_nl, dAf, dI_E, dI_F, dHE, dProtein, dWool, dLipid),
       FEC = as.numeric(FEC), E_I = as.numeric(E_I), kF_I = as.numeric(kF_I),
       EB = as.numeric(EB), Food_intake = as.numeric(Food_intake), EBW = as.numeri
c(EBW),
       BW = as.numeric(BW), fat_thick = as.numeric(fat_thick))
  }) # end with(as.list ...
}
```

Default parameters

Initial values have to specified for the different state variables.

```
### DEFAULT PARAMETER ##################
parmsInfGrow_default <- list(
  E0 = 0.7, thauLI = 2, kLE = 2, thauLE = 15, kA = 0.62, kF0 = 0.11, muLE = 0.01,
muA = 0.015, sex_ratio = 0.5, FEC_i = 7000,
  betaHE = 0.16, HE0 = 35, kHE_LE = 0.00015, kHE_Anf = 0.0005, kHE_Af = 0.0011,
  betaI = 0.05, rhoI_E = 0, rhoI_F = 0, I_E0.5 = 5, I_F0.5 = 5, LI0.5 = 3000, LE0.
5 = 1500, I_E0 = 1e-6, I_F0 = 0, e_IE = 0, e_IF = 0,
  beta_Protein = 0.27, AshtoProtein_ratio = 0.211, WatertoProtein_ratio = 3.25, be
ta_Water = 0.815,
  bl = 50, blc = 39.6, bp = 56, e_maint = 1.63, DM = 0.888, EEC = 7.7, dDM = 0.76,
  bLipid_0 = -4.0120, bLipid_FT = 0.5597,  bLipid_EBW = 1.523453,
  B_Protein = 0.023, Protein_m = 6.76, Lipid_m = 14, K_Wool = 0.001)
```

Initial values

Initial values have to specified for the different state variables. NB : some initial values that are also used during the simulations are specified in the default parameters.

```
cinit <- c(LI = 10000, LE = 0, Am = 0, Af_nl = 0, Af = 0,
         I_E = parmsInfGrow_default$I_E0, I_F = parmsInfGrow_default$I_F0,
         HE = parmsInfGrow_default$HE0, Protein = 4.81, Wool = 0.77, Lipid = 7.67)
```

Run a simulation

To run a simulation we define an hypothetical scenario with a constant food intake of 1.9kg per day and equivalent to 30g of food intake per kg of body weight. Real-time series can be used instead and then smoothed using the 'smooth.spline' function or linear regression.

```
datadef <- data.frame(time = 1:35, Food_intake = 1.9, Food_intake_prop = 0.03)
interpol <- with(datadef, smooth.spline(time, Food_intake, df = 7))
interpol2 <- lm(Food_intake_prop ~ time, datadef)
```

Simulation is run with the 'ode' function of deSolve and results are stored in the matrix 'out'.

```
out <- ode(y = cinit, times = seq(0, 35, 0.1), func = InfGrow_model, parms = parms
InfGrow_default)
```

Visualization of outputs.

```
head(out)

##      time        LI LE Am Af_nl Af   I_E I_F HE  Protein      Wool    Lipid FEC
## [1,]  0.0 10000.000  0  0     0  0 1e-06   0 35 4.810000 0.7700000 7.670000   0
## [2,]  0.1  9823.240  0  0     0  0 1e-06   0 35 4.812246 0.7704811 7.683566   0
## [3,]  0.2  9649.608  0  0     0  0 1e-06   0 35 4.814491 0.7709624 7.697129   0
## [4,]  0.3  9479.038  0  0     0  0 1e-06   0 35 4.816733 0.7714440 7.710691   0
## [5,]  0.4  9311.491  0  0     0  0 1e-06   0 35 4.818973 0.7719258 7.724249   0
## [6,]  0.5  9146.904  0  0     0  0 1e-06   0 35 4.821212 0.7724078 7.737806   0
##      E_I kF_I       EB Food_intake      EBW       BW fat_thick
## [1,]   1    1 6.783518         1.9 30.14328 39.74451  4.652567
## [2,]   1    1 6.782346         1.9 30.16590 39.77422  4.657759
## [3,]   1    1 6.781176         1.9 30.18852 39.80391  4.662940
## [4,]   1    1 6.780008         1.9 30.21112 39.83358  4.668110
## [5,]   1    1 6.778842         1.9 30.23371 39.86324  4.673268
## [6,]   1    1 6.777677         1.9 30.25628 39.89289  4.678417

tail(out)

##        time           LI         LE       Am    Af_nl       Af   I_E I_F
## [346,] 34.5 1.248194e-27 0.02619599 2133.022 304.0864 1828.935 1e-06   0
## [347,] 34.6 1.003873e-27 0.02459655 2129.825 300.3098 1829.515 1e-06   0
## [348,] 34.7 8.073752e-28 0.02309477 2126.634 296.5800 1830.054 1e-06   0
## [349,] 34.8 6.493399e-28 0.02168469 2123.447 292.8965 1830.550 1e-06   0
## [350,] 34.9 5.222383e-28 0.02036069 2120.265 289.2588 1831.006 1e-06   0
## [351,] 35.0 4.200156e-28 0.01911754 2117.087 285.6661 1831.421 1e-06   0
##              HE  Protein      Wool    Lipid      FEC E_I kF_I       EB
## [346,] 15.37562 5.468992 0.9479650 12.23359 28075.76   1    1 6.472879
## [347,] 15.36678 5.470582 0.9485120 12.24653 28084.67   1    1 6.472206
## [348,] 15.35837 5.472171 0.9490591 12.25948 28092.93   1    1 6.471535
## [349,] 15.35038 5.473758 0.9496064 12.27242 28100.55   1    1 6.470864
## [350,] 15.34280 5.475343 0.9501539 12.28536 28107.55   1    1 6.470195
## [351,] 15.33564 5.476927 0.9507015 12.29830 28113.92   1    1 6.469526
##        Food_intake      EBW       BW fat_thick
## [346,]         1.9 37.34147 49.22787  5.981572
## [347,]         1.9 37.36073 49.25333  5.984484
## [348,]         1.9 37.37997 49.27877  5.987392
## [349,]         1.9 37.39920 49.30420  5.990296
## [350,]         1.9 37.41843 49.32963  5.993196
## [351,]         1.9 37.43765 49.35504  5.996093
```

10 Appendix2: Report for the AQAL goat allocation model

AQAL is a mechanistic model, primarily developed for dairy cows, that simulates trajectories of phenotypes throughout lifetime, depending on trajectories of resource acquisition and allocation, driven by four genetic-scaling parameters, and depending on the nutritional environment (quantity and quality of feed resources) (Puillet et al., 2016). Because the model depends on trajectories of resource acquisition and allocation, and not on complex biological processes, we aimed to convert the already calibrated AQAL cow into a AQAL goat version using goats 'life functions trajectories available in the literature. For this, as a first step, we are checking and when necessary, adapting the equations that describe the trajectories of energy acquisition and allocation into "products" (structural mass, labile mass, body mass, soma, and maintenance) for a goat female non-lactating and non-pregnant. As soon as we can simulate a female non-lactating and non-pregnant growth trajectory, we start exploring the parameters related to describe the trajectories of energy and products related to reproduction and lactation. For the reproductive phase we have data from two research stations, Grignon and Bourges. At both stations we have animals from the divergent lines for longevity. For the first part calibrating growth trajectories, we are using papers that have measured and described the trajectories of intake (DM and energy) and body components (mass, fat, protein, and energy) and parameters that convert this energy allocated as products into metabolizable and net energy (Castagnino et al., 2015; Härter et al., 2016; Härter et al., 2017; Souza et al., 2017; Noziere et al., 2018; Almeida et al., 2019; Souza et al., 2020). We are also using real data from the INRAE farm, in Grignon to visually drive all the updates in the model.

Until this moment, we have updated the parameters that drive basal acquisition (kg DM/d; from 7 to 1.5 kg/d), energy transfer rate from soma to growth (from 0.0024 to 0.004), efficiency of maintenance (NE/ME; from 0.65 to 0.63), basal acquisition at birth (kg DM/d; from 2 to 0.2), parameter of basal acquisition logistic function (from 0.012 to 0.02), body mass at birth (kg; from 42.8 to 3), and fixed cost of maintenance (net energy kcal/kg $EBW^{0.75}$; from 93 kcal/kg $BW^{0.75}$ to 63.6 kcal/kg $EBW^{0.75}$). After the updates, we already can simulate the trajectories of basal DM acquisition (Figure 1), close to what is observed in the real data of the INRAE farm, predicted using the equation proposed by Almeida et al. (2019). We also tried to simulated BW and BCE and they have been overpredicted by the model (Figure 2). So, at this step, we checking the parameters related to structural mass (flow of energy, efficiencies, body compositions, and energy allocated according to body composition using the equations proposed by (Souza et al., 2017; Souza et al., 2020)).

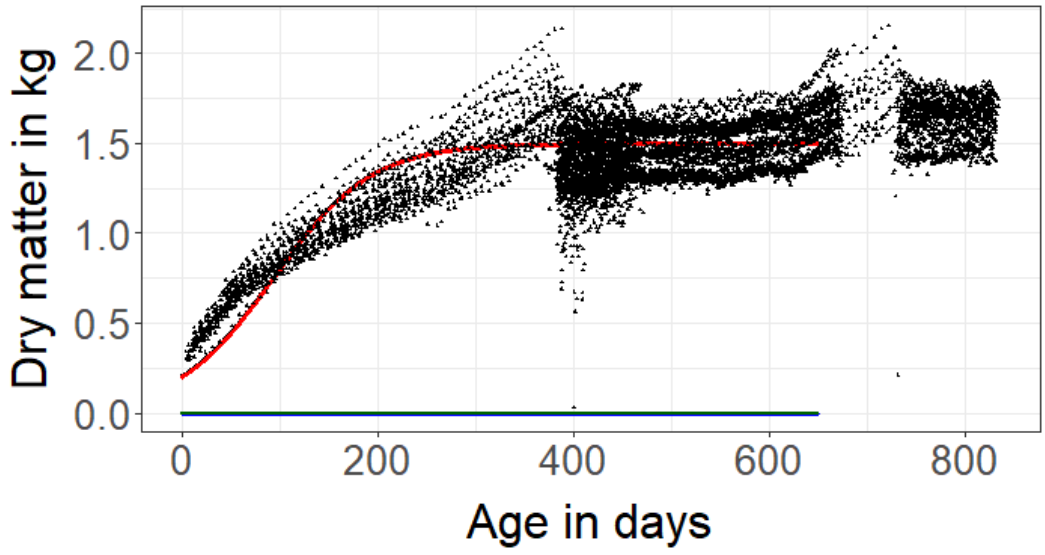

Figure 1: Dry matter intake (kg/d) simulated using the ADAL model (red line) and predicted using the equation DMI (g/d) = $98.3BW^{0.681}$, in which BW is from real data recoded at the INRAE farm (black dots).

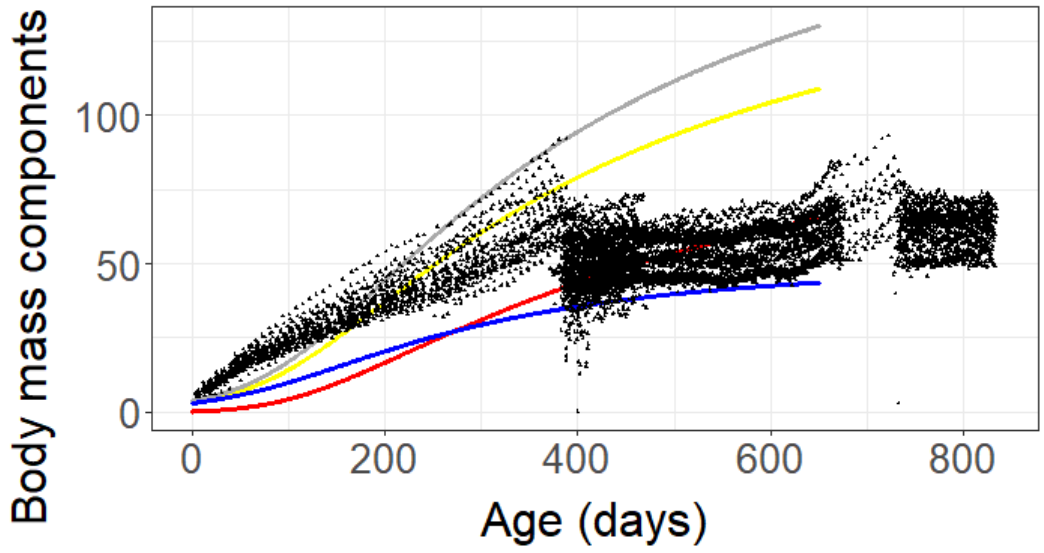

Figure 2: Total body weight (kg; grey line), empty body weight (kg; yellow line), reserves (kg; red line), and structural mass (kg; blue line) simulated by the AQAL model and body weight observed in the INRAE farm (black dots).

References

Almeida, A.K. de, L.O. Tedeschi, K.T. de Resende, B. Biagioli, A. Cannas, and I.A.M. de A. Teixeira. 2019. Prediction of voluntary dry matter intake in stall fed growing goats. Livest. Sci. 219:1–9. doi:10.1016/j.livsci.2018.11.002.

Castagnino, D.D.S., C.J. Härter, A.R. Rivera, L.D. De, H. Giovane, D.O. Silva, B. Biagioli, and K.T. De Resende. 2015. Revista Brasileira de Zootecnia Changes in maternal body composition and metabolism of dairy goats during pregnancy 44:92–102.

Härter, C.J., J.L. Ellis, J. France, K.T. Resende, and I.A.M.A. Teixeira. 2016. Net energy and protein requirements for pregnancy differ between goats and sheep. J. Anim. Sci. 94:2460–2470. doi:10.2527/jas.2015-9673.

Härter, C.J., L.D. Lima, H.G.O. Silva, D.S. Castagnino, A.R. Rivera, K.T. Resende, and I.A.M.A. Teixeira. 2017. Energy and protein requirements for maintenance of dairy goats during pregnancy and their efficiencies of use. J. Anim. Sci. 95:4181–4193. doi:10.2527/jas.2017.1490.

Noziere, P., D. Sauvant, and L. Delaby. 2018. INRA Feeding System for Ruminants. Wageningen Academic Publishers, The Netherlands.

Puillet, L., D. Réale, and N.C. Friggens. 2016. Disentangling the relative roles of resource acquisition and allocation on animal feed efficiency: Insights from a dairy cow model. Genet. Sel. Evol. 48:1–16. doi:10.1186/s12711-016-0251-8.

Souza, A.P., N.R. St-Pierre, M.H.M.R. Fernandes, A.K. Almeida, J.A.C. Vargas, K.T. Resende, and I.A.M.A. Teixeira. 2020. Energy requirements and efficiency of energy utilization in growing dairy goats of different sexes. J. Dairy Sci. 103:272–281. doi:10.3168/jds.2018-15930.

Souza, A.P., N.R. St-Pierre, M.H.R.M. Fernandes, A.K. Almeida, J.A.C. Vargas, K.T. Resende, and I.A.M.A. Teixeira. 2017. Sex effects on net protein and energy requirements for growth of Saanen goats. J. Dairy Sci. 100:4574–4586. doi:10.3168/jds.2016-11895.